Computers, Environment and Urban Systems 34 (2010) 179–188

Contents lists available at ScienceDirect

Computers, Environment and Urban Systems

journal homepage: www.elsevier.com/locate/compenvurbsys

LiDAR assisted emergency response: Detection of transport network obstructions caused by major disasters

Mei-Po Kwan *, Daniel M. Ransberger

Department of Geography, The Ohio State University, Columbus, OH 43210-1361, USA

ARTICLE INFO

Article history:
Received 27 March 2009
Received in revised form 12 January 2010
Accepted 7 February 2010

Keywords:
Emergency response
Hurricane Katrina
LiDAR
Transport network obstructions

ABSTRACT

This article explores whether the use of LiDAR data in detecting transport network obstructions shortens the time required to reach disaster sites. It presents a method for doing this using LiDAR data collected in New Orleans, Louisiana (USA) before and after Hurricane Katrina. It involves identifying all the LiDAR data points that lie within transport links (e.g., highways or streets) and performing blockage detection analysis with the Quick Terrain Modeler (QT Modeler) software. After performing this blockage detection, routing analysis was performed to determine the effect of these obstructions on the time needed to reach 30 randomly chosen locations in the study area from the centrally located City of New Orleans Fire Station. The results show that the use of LiDAR data in emergency response situations can significantly reduce the response times for first responders to reach disaster sites.

1. Introduction

Globally, the number of disasters and the number of people affected by them have been steadily increasing. According to the 2007 World Disasters Report, 427 natural disasters and 297 technological disasters were reported worldwide in 2006. As a result of these disasters, 33,733 people were killed and 1.43 million people were injured or suffered some form of economic loss (Walter, 2007). In the United States, over 1200 disasters had occurred from 1987 to 2006, claiming the lives of nearly 10,600 people and affecting 11.5 million people. The cost of disasters has also been increasing, with Hurricane Katrina responsible for the highest damages (estimated to be US$129 billion) ever reported for one single disaster (Hoyois, Scheuren, Below, & Guha-Sapir, 2007).

With this increasing number of disasters, emergency management continues to play a crucial role in planning for, responding to and mitigating against the often devastating impact of these events. In the United States, emergency management agencies such as the Federal Emergency Management Agency (FEMA) are tasked with the mission to plan for and respond to disasters. In recent years, both natural and "human-made" disasters have underscored the need for these agencies to be able to promptly and effectively respond to different kinds of emergencies.

Geospatial technologies that enable the collection of accurate and timely data of disasters have considerable promise to facilitate emergency response. One technology that has received considerable attention recently is Light Detection and Ranging (LiDAR). When coupled with GPS, this technology enables the building of highly accurate three-dimensional (3D) models of the Earth's surface at lower costs relative to other traditional remote sensing methods. This type of data collection has numerous potential applications in emergency management, environmental monitoring and land use analysis. Because it is a relatively new technology when compared to aerial and satellite photography, there are still many applications that have yet to be explored.

This study explores whether the use and analysis of LiDAR data in detecting transport network obstructions during emergency response shortens the time first responders reach disaster sites. We present a method for doing this using LiDAR data collected in New Orleans, Louisiana (USA) before and after Hurricane Katrina. It involves identifying all the LiDAR data points that lie within transport links (e.g., highways or streets) and performing blockage detection analysis with the Quick Terrain Modeler (QT Modeler) software. After performing this blockage detection and incorporating the obstructions data into a transport network GIS database, routing analyses were performed to determine the effect of these obstructions on the time needed to reach 30 randomly chosen locations in the study area from the centrally located City of New Orleans Fire Station. The study shows that the use of LiDAR data in emergency response situations can significantly reduce the response time for first responders to reach disaster sites.

2. Emergency management and geospatial technologies

The damages, injuries, and deaths as a result of natural and human-made disasters have seen a steady increase over the last

* Corresponding author. Tel.: +1 614 292 9465; fax: +1 614 292 6213.
E-mail address: kwan.8@osu.edu (M.-P. Kwan).

0198-9715/$ - see front matter © 2010 Elsevier Ltd. All rights reserved.
doi:10.1016/j.compenvurbsys.2010.02.001

20 years (Cutter, 2003). This has increased the need to develop effective methods for managing and responding to these disasters. GIS have been used by emergency managers as a valuable tool in emergency response in various kinds of disasters, including floods, bushfires, droughts, hailstorms, tsunamis, hurricanes, landslides, and earthquakes (e.g., Abbas, Srivastava, Tiwari, & Bala Ramudu, 2009; Aitkenhead, Lumsdon, & Miller, 2007; Ball & Guertin, 1992; Chen, Blong, & Jacobson, 2003; Chou, 1992; Corbley, 1995; Dash, 1997; Ertug Gunes & Kovel, 2000; Kaiser, Spiegel, Henderson, & Gerber, 2003; Radke et al., 2000). GIS have many capabilities to process, analyze and display spatial information for emergency response personnel, enabling them to make faster and better-informed decisions than by using traditional paper maps (Cova, 1999; Goodchild, 2003; Kwan, 2003). By coupling data such as 3D elevation models or underground water infrastructure with roads and highways, emergency managers are able to have a more comprehensive view of the impact of disasters through interactive geovisualization.

A large number of GIS applications for emergency management have been developed to date (e.g., Dunn & Newton, 1992; Carrara & Guzzetti, 1996; Chen et al., 2003; van Oosterom, Zlatanova, & Fendel, 2005). One early example is the GIS developed by the South Florida Water Management District for routine and emergency management of water resources (Corbley, 1995). In the immediate aftermath of Hurricane Andrew which struck in 1992, the GIS was used to automatically generate maps to facilitate various emergency response tasks, including guiding disaster relief efforts, tracking debris pickup to keep the canals flowing, and monitoring burn sites to prevent hazardous waste being washed into canals (Cova, 1999). As most landmarks had been destroyed by the hurricane, the GIS's capability to generate transport network data had proven to be highly valuable in responding to the effects of the hurricane (Corbley, 1995; Cova, 1999).

In the case of the World Trade Center attacks in 2001, the use of GIS was also extensive during the initial rescue and relief operations (Bruzewicz, 2003; Cahan & Ball, 2002). As Sean Ahearn (2003) recalled, the full range of mapping science technologies was deployed in this case, including GIS, GPS, and remote sensing. Soon after the attacks on September 11, 2001, a large quantity of imagery was collected including high- and medium-resolution satellite imagery, thermal infrared, high-resolution panchromatic digital serial imagery, LiDAR, and hyperspectral data (Bruzewicz, 2003). Some early images acquired on September 12 show considerable detail on the site and were helpful for assessing the damage and guiding rescue efforts.

GIS were also widely used in the response and recovery phases for Hurricane Katrina in 2005. Five days after Katrina hit the Gulf Coast, FEMA and Louisiana State University (LSU) personnel worked jointly to establish the LSU GIS Clearinghouse Cooperative (LGCC) (Mills et al., 2008). The primary purpose of the clearinghouse is to organize, disseminate and archive geospatial information related to Hurricane Katrina. As Susan Cutter (2003) points out, "In heavily damaged areas, such as hurricane-affected coasts or cities damaged by earthquakes, it is often difficult to assess precise locations as most buildings and landmarks have been destroyed. GPS, coupled with GIS and remote sensing data have been employed to assist in compiling quick damage estimates." In the case of Hurricane Katrina, the most common types of requests "were from pilots needing imagery of the New Orleans central business district, coordinates of buildings where people had gathered and now needed rescue, and data on tower locations that could be obstacles on the flight path" (Curtis, Mills, Blackburn, & Pine, 2006). A large number of requests to keep the data on locations of flooded and passable roads up-to-date were also received (Curtis et al., 2006).

While Hurricane Andrew, the World Trade Center attacks and Hurricane Katrina are some recent examples of GIS applications in emergency response, considerable research has been devoted to the creation of spatial decision support systems that enable emergency managers to make informed decisions and help first responders to reach disaster sites as quickly as possible (e.g., Abbas et al., 2009; Dunn & Newton, 1992; Maniruzzaman, Okabe, & Asami, 2001; Mansourian, Rajabifard, & Zoej, 2005; Pu & Zlatanova, 2005; Zerger & Smith, 2003). Cova and Church (1997), for instance, developed a critical cluster model for identifying neighborhoods that may face transportation difficulties during an evacuation using GIS. Aitkenhead et al. (2007) used remote sensing-based neural network mapping to assess tsunami damage and identify areas that were inaccessible by road. Kwan and Lee (2005) developed a GIS-based Intelligent Emergency Response System (GIERS) that utilizes 3D models of buildings and Intelligent Transportation Systems (ITS) to improve emergency response times in multi-level structures (e.g., multi-story buildings like the World Trade Center).

Building upon these earlier works, this study seeks to contribute to research on the use of LiDAR to assist emergency managers to make better decisions. Past studies have used LiDAR in emergency preparedness, mitigation and response. One study developed a methodology for determining preferable disaster and hurricane evacuation routes in North Carolina (Laefer & Pradhan, 2006). It utilized LiDAR data to predict areas where debris would be likely to fall onto roads as a result of heavy winds from a hurricane or other storm. The authors measured the tree heights using LiDAR data, and then used those heights and measures of distance from the road to the base of the tree to predict whether it would block the highway if the tree were to fall. This allowed the researchers to determine which highways would be least likely to be impacted by falling trees and subsequently identify those as preferable evacuation routes. This study illustrates how LiDAR can be used in disaster planning and mitigation by identifying the least hazardous routes.

Emergency managers have also used LiDAR data in active disaster response situations. When responding to the attacks on the World Trade Center in New York City, LiDAR data were collected on a daily basis for almost 2 weeks after the attacks (Cahan & Ball, 2002). In the initial response, LiDAR was used to acquire images of the Ground Zero area since it could penetrate the thick smoke clouds emanating from the debris pile. Firefighters and other responders also used the LiDAR imagery to form an enhanced mental picture of the disasters site (Ahearn, 2003). LiDAR has also been used before and after hurricanes, including Hurricane Katrina and Hurricane Rita in 2005, and more recently Hurricane Ike in 2008 (Center for Coastal, 2007; Center for Coastal, 2008a; Center for Coastal, 2008b).

Other studies have conducted comparative analyses that utilized LiDAR for rapid change detection. Armenakis and Savopol (2004) used pre- and post-event geospatial data, primarily LiDAR data, in a change analysis for monitoring and tracking the type and rate of landscape changes. They concluded that 3D visualizations of the disaster area can improve emergency managers' understanding of the situation, and enable them to make better plans and decisions. They also found that because LiDAR data can be collected relatively quickly and time is crucial in emergency situations, LiDAR data are an effective tool that can be used for "mapping, modeling, change detection, and monitoring and visualization tools for knowledge-based decision-making" (Armenakis & Savopol, 2004).

Since LiDAR data can be acquired at very high resolution (15 cm) and the process is highly automated, utilizing LiDAR has benefits over the more traditional photogrammetric method of remote sensing (Baltsavias, 1999). LiDAR is also not as dependent on the weather as photogrammetry. Data can be acquired during the

day or night, as compared to aerial photography which can only be acquired during the day and only when the weather and sun angle meet optimal conditions. LiDAR is also able to acquire imagery and models of the Earth's surface even when it is obstructed from view of aerial photography by smoke. For example, in the response to the attacks on the World Trade Center in New York City, responders found LiDAR to be especially helpful during the initial response phase when aerial photos were partially obscured by smoke from the debris pile (Huyck & Adams, 2002). Another advantage is that LiDAR is capable of acquiring data at higher altitudes than traditional aerial photography while maintaining accuracy. Also, as compared to aerial photography, LiDAR data are already geographically referenced, and having the remote sensing data already in this form saves the time that would normally be required to orthorectify the imagery collected (Baltsavias, 1999).

3. Data and method

This study examines whether using LiDAR data in detecting and taking into account transport network obstructions during emergency response shortens the time required to reach disaster sites. This is a critical area that needs more research given that federal agencies responsible for emergency response (such as FEMA) have been criticized in recent years for what some have considered an unacceptable and poorly executed response to the aftermath caused by Hurricane Katrina. LiDAR has the capability of quickly assessing the amount of damage that has been sustained by the transport network as the result of a disaster (Biasion, Bornaz, & Rinaudo, 2005; Firchau & Wiechert, 2005). Depending on the technology used, these systems are able to survey large areas quickly and more efficiently than deploying emergency responders to drive over every part of a transportation network to ascertain the locations of debris, damage, and other blockages of the transport network. This section describes the data and method of the study, while the results will be presented in the next section.

3.1. Study area

The city of New Orleans, Louisiana was selected as the study area and the disaster event chosen for analysis was Hurricane Katrina. These particular selections were made because of the scale of the event and the number of people affected, and there is a considerable amount of data available for the New Orleans area from various sources. These data include vector data (e.g., street centerlines, administrative boundaries, and parcels) and remotely sensed data (e.g., LiDAR, aerial imagery, and satellite imagery).

New Orleans is located in the southeastern part of the state of Louisiana (USA) and is the largest city in that state (Fig. 1). It also shares a designation as Orleans Parish (parishes in Louisiana are the equivalent of counties in other states in the US). To the north of the city is Lake Pontchartrain, while the Mississippi River flows through the southern and downtown areas of the city. The city is approximately 110 miles from the Gulf of Mexico. Portions of the city sit below sea level, and because of this there is a network of levees and canals that are meant to serve to keep the city from flooding. As of the 2000 census, the City of New Orleans had a population of 484,674.

3.2. Data

This study used the LiDAR datasets collected before and after Hurricane Katrina by the US Geological Survey and Louisiana State University (LSU). LiDAR is similar in concept to Radar. Airborne LiDAR systems have a laser and sensor which are mounted in an aircraft. The laser emits a pulse, or a narrow laser beam, toward the ground. The sensor then receives the pulses as they are reflected off the ground and back toward the aircraft. This process is usually

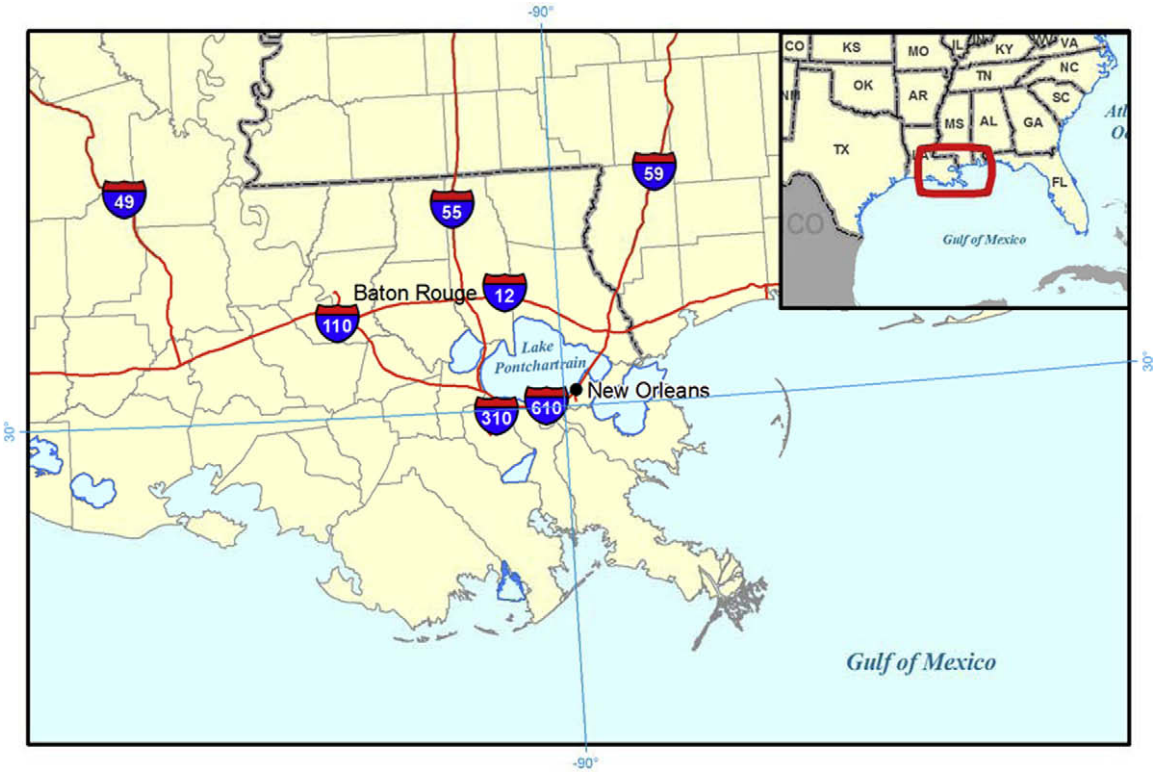

Fig. 1. The study area: New Orleans, Louisiana (USA).

accomplished with an opto-mechanical scanning assembly with scanning mirrors that generate the swath of laser pulses fired at the ground. After a pulse has been sent and received, the range can be determined by calculating the time-of-flight of that pulse, or the amount of time it took for the laser pulse to travel from the aircraft to the ground and then bounce back to the sensor in the aircraft.

In addition to the laser and sensor assembly, the aircraft is equipped with a Global Positioning System (GPS) receiver to record the aircraft's latitude, longitude and altitude, as well as an Inertial Measurement Unit (IMU) to record the aircraft's levels of yaw, pitch, and roll at a given moment. Measurements from the GPS and IMU are coupled with the instantaneous mirror angle of the laser assembly and the range of a particular fired pulse. All of these variables are used to determine an accurate three-dimensional ground position, including *X*, *Y* and *Z* measures. The level of accuracy that can be achieved will be about 15 cm for each LiDAR point (Centre for Applied Remote Sensing Modelling & Simulation, 2006).

The US Geological Survey and Louisiana State University (LSU) have collected LiDAR datasets both before and after Hurricane Katrina. For this research, pre-storm LiDAR data were obtained from the LSU's "Atlas: Louisiana Statewide GIS" website at http://atlas.lsu.edu/LiDAR. This dataset was collected in March 2003 and has a resolution of 0.14 m. It includes basic LiDAR attributes of *X*, *Y* and *Z* (elevation) coordinates, but does not include intensity or other attributes. The horizontal data are provided in the Universal Transverse Mercator (UTM) Zone 15 North coordinate system using the North American Datum of 1983 (NAD83). The vertical (elevation) data are provided using the North American Vertical Datum of 1988 (NAVD88) with units of survey feet. This LiDAR dataset covers the entire New Orleans area. As shown in Fig. 2 where the downtown New Orleans area is clearly represented, one can identifies the major structures in the downtown area, including the Superdome, the high-rise buildings in the central business district, and the highways and other parts of the transportation network.

The post-storm LiDAR data were obtained from the USGS's disaster data repository, available at http://gisdata.usgs.net/hurricanes/katrina/index.php (United States Geological Survey, 2006). This dataset was collected during September 1–8, 2005 and has a resolution of 0.14 m. It includes the *X*, *Y*, and *Z* coordinates, intensity of the return, and date and time of acquisition of each point. The horizontal data are provided in the geographic coordinate system using latitude and longitude coordinates, using the North American Datum 1983 (NAD83). The elevation data are also provided using the NAVD88 in meters. This set of data, however, does not have full coverage of the entire New Orleans area. It was collected along the southern shore of Lake Pontchartrain and the areas where levees are located. It covers approximately one mile inland from the southern shore of Lake Pontchartrain, and runs along the entire coastal area that is within the New Orleans city boundary. The analyses and results reported in this paper are based on this area (Fig. 3).

In addition to the pre-storm and post-storm LiDAR data (with a total of over 50 million LiDAR data points), relevant vector data were obtained from the City of New Orleans GIS (2008) via their GIS portal on the web. The most important among them are street centerlines of the study area, which were last updated in October 2006. These street centerlines were used to identify all the LiDAR data points that lie within transport links (e.g., highways or streets). They were also used to perform the routing analysis in this study.

3.3. Pre-analysis data preparation

Because the pre-storm and post-storm LiDAR data were provided in different coordinate systems, one of them had to be transformed to match the coordinate system of the other. Because the Quick Terrain Modeler (QT Modeler) software used in this study is optimized for the UTM coordinate system, the post-storm data were first transformed from the latitude and longitude coordinate system to UTM. Further, since the pre-storm data set had its elevation data in survey feet units while the post-storm data used

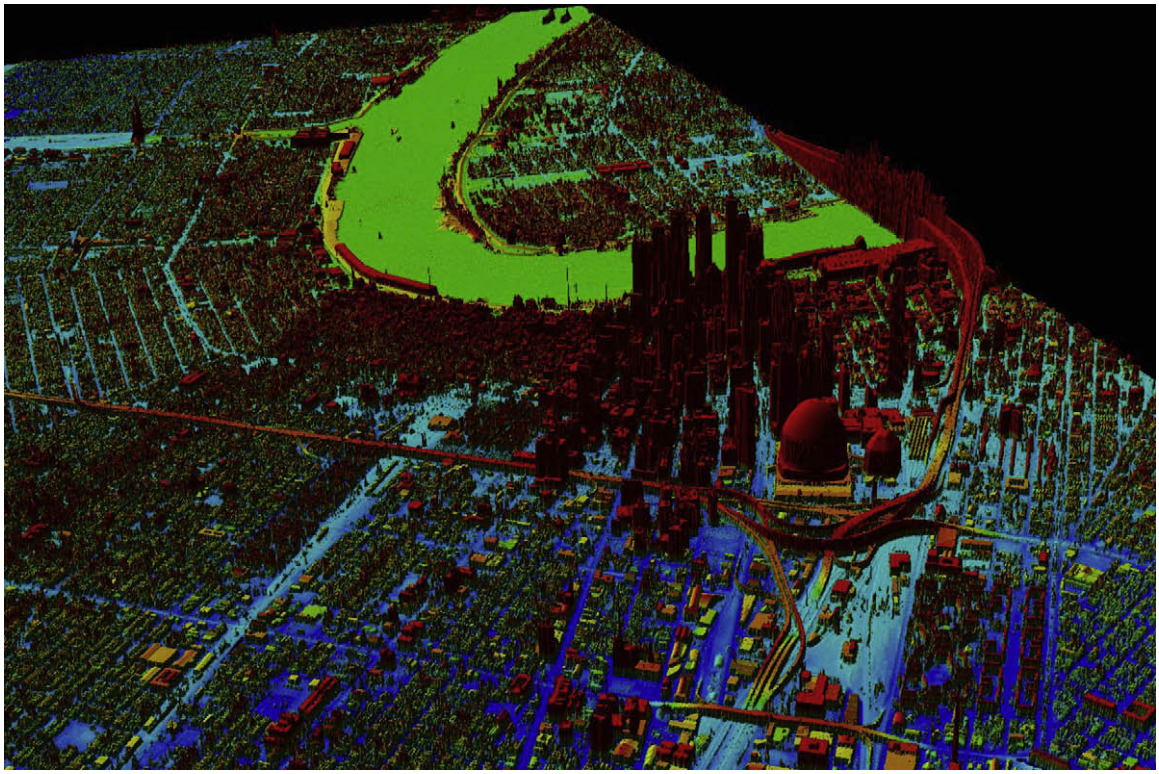

Fig. 2. 3D surface representation of downtown New Orleans, LA created from LiDAR data.

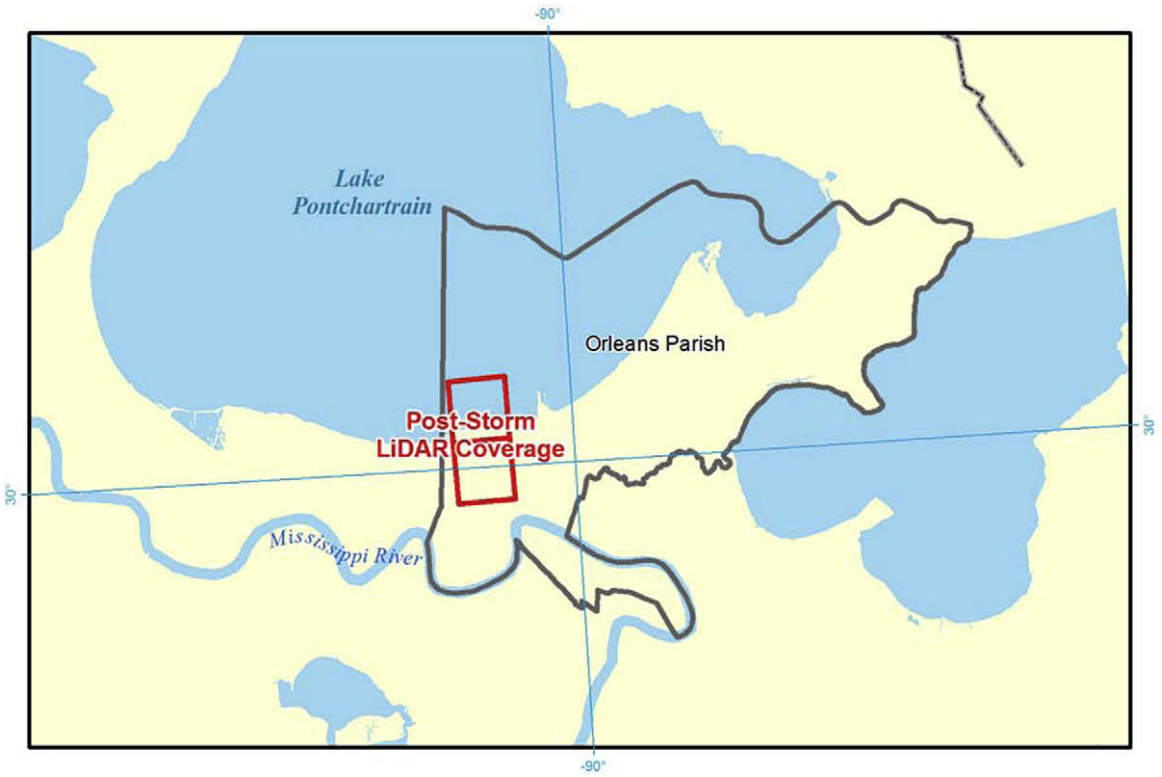

Fig. 3. Coverage of post-storm LiDAR data in the New Orleans area.

meters, the pre-storm elevation units were converted from survey feet to meters so that the units of measure were consistent across the pre- and post-storm datasets.

Since transport network obstructions will be determined based on the changes in elevation between the pre-storm and the post-storm LiDAR data, all the LiDAR data points that lie within transport links (e.g., highway or street) need to be identified and extracted. This was done using the vector road network data obtained from the City of New Orleans GIS Data Portal. A buffer layer was created in ArcGIS to take into account the width of the roads, with a 30-foot buffer for highways and a 20-foot buffer for residential and other streets. All LiDAR points that were completely within the road buffer polygons were selected. This extraction process was applied for both pre- and post-storm data.

3.4. Detection of transport network obstructions

Once the LiDAR points on the road network were selected, the pre- and post-storm data files were imported into QT Modeler and converted to digital elevation models (DEMs). Since any debris or other road blockages would be detectable by changes in elevation between the pre- and post-storm data, these DEMs were used to perform a change detection analysis with the built-in elevation change detection function in QT Modeler. The elevation change detection tool requires a range of heights to be input. For these LiDAR data, an increase of 5 m to a decrease of 5 m was selected.[1] This allowed for the detection of moderately sized pieces of debris that would likely take a large amount of effort to clear from the roadway to make it passable. The change detection tool used this range to color the 3D surface to show where elevation change was detected. Markers were then placed at all locations with a 2.5–5-m increase in elevation that spanned the entire width of the road. These markers were then exported to a shapefile and incorporated into a post-storm street network created in ArcGIS.

3.5. Pre-storm and post-storm routing analysis

The street network data from the City of New Orleans GIS was utilized to set up a pre-storm street network using the Network Analyst extension of ArcGIS. The streets file contains all of the attributes required to model the street network for the city. These attributes include a one-way street indicator, the direction of travel if it is one-way, the speed limit on a particular street segment, and the length of the segment. They were used to model all possible turns in the network to determine network connectivity and possible directions of travel. After the pre-storm transport network was set up, shortest path calculation was performed to determine the amount of time required to travel from the City of New Orleans Fire Station, located at 987 Robert E. Lee Blvd., to 30 randomly selected locations in the study area (Fig. 4).[2] The optimal route under normal conditions (pre-storm) and the travel time required were

[1] Whether these elevation changes were actually caused by debris or some other causes (e.g., parked or moving cars) cannot be determine by using the LiDAR data alone. While high-resolution aerial photos or satellite images can be used to verify each obstruction point identified by the LiDAR data, it is fraught with difficulties since these images were likely to be taken at different times or dates when compared with the LiDAR data. Our analysis of post-storm transport network obstructions included only those LiDAR points with a 2.5–5 m increase in elevation that spanned the entire width of the road. This would likely ensure that those were "major" obstructions caused by debris, flooding, and destroyed structural components.

[2] The random selection of 30 addresses is based on an important property of the sampling distribution of the mean (known as the central limit theorem): if a random sample of n observation is selected from any population, the sampling distribution of the mean tends to approximate the normal distribution when the sample size is sufficiently large regardless of the underlying distribution. Although the larger the sample size, the better will be the normal approximation to the sampling distribution of the mean, the rule of thumb is that a sample size of at least 30 will suffice. Using a sample size of 30 would thus help satisfy the normal distribution assumption of many statistical tests.

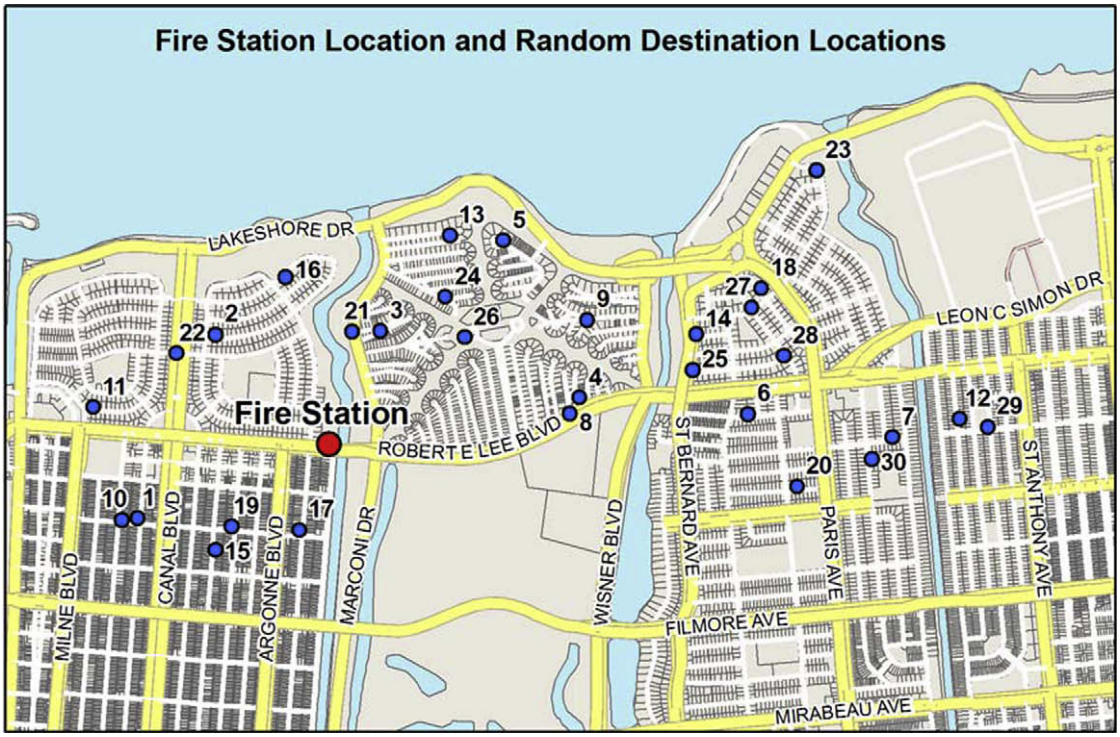

Fig. 4. Location of the City of New Orleans Fire Station and the 30 randomly chosen locations in the study area.

determined for each of the 30 locations using Dijkstra's shortest path algorithm and the highest speed allowed for each street segment.

The network blockages identified by the LiDAR data were then used to construct a post-storm transport network and two new routes were calculated for each location. The first route assumed that emergency responders traveling to a particular address had no knowledge of the locations of blockages in the transport network. Therefore, they would initially leave the fire station as if they were traveling the optimal route that existed before the storm, and each time the crew encountered a blockage they would need to turn around and find another unblocked road until they finally reach their location. This process is henceforth termed Naïve Blockage Re-routing. The second route that was calculated assumed that the LiDAR data had been collected and analyzed for blockages and had been incorporated into the street network database. This means that the routing calculation would take these blockages into account and would attempt to identify routes that avoid these blockages. This type of routing is henceforth termed LiDAR Assisted Blockage Re-routing.

For both Naïve and LiDAR Assisted Blockage Re-routing calculation, we did not modify the travel speed for different types of transport links to take into account other minor or real-time obstructions. While the assumption of free-flow traffic is unrealistic for the post-storm calculation (since there may be other vehicles and objects that were not identified as obstructions by the LiDAR data on the streets), we hesitate to make assumptions about the spatial pattern of other minor obstructions that would have reduced travel speed (since these blockages are highly unpredictable and can be rapidly changing in real-time). If these other minor obstructions were widespread in the study area, we can assume that there was a general reduction in travel speed that did not significantly change the topological structure of the transport network. In other words, slower travel speeds throughout the network would lead to longer travel times but would not change the shortest paths identified in the routing analysis reported in the next section. In light of this, the results presented in this paper represent the "best scenario," where only major network obstructions (those with a 2.5–5-m increase in elevation that spanned the entire street or highway) were considered. It can also be considered a "LiDAR-only scenario," which aims at isolating the contribution of a LiDAR-based routing analysis without using additional data layers (such as high-resolution satellite images or aerial photos) to identify minor network obstructions or to derive alternative travel speed scenarios.

4. Results

4.1. Detection of network obstructions

Using the pre-storm and post-storm DEMs derived from the LiDAR data and the elevation change detection tool of QT Modeler, 86 network obstructions were identified. These locations were characterized by an increase in elevation from 2.5 to 5 m that spanned the entire street or highway. They are locations with deposits of large debris on the streets that present considerable difficulty for emergency vehicles attempting to reach citizens who might be injured or stranded as a result of the storm. As indicated in Fig. 5, which shows the 86 detected blockages overlaid on a street map of New Orleans, the obstructions were widespread throughout the study area. These obstructions have the effect of making many parts of the street network impassable by emergency vehicles. The blockages inventory was used in the routing analysis described as follows.

4.2. Routing analysis

To evaluate the effect of these network obstructions on travel time and distance, the shortest path from the City of New Orleans Fire Station to each of the 30 randomly chosen addresses was determined under three response conditions: under normal (pre-storm) conditions where no debris is present; under post-storm

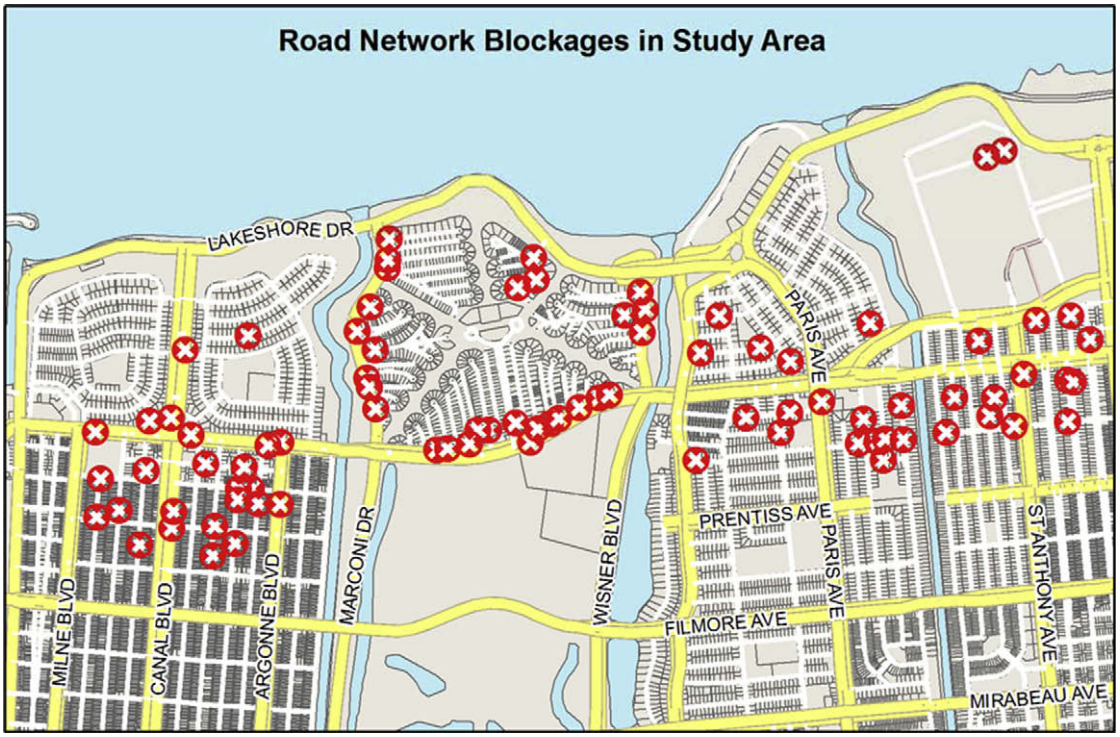

Fig. 5. Post-storm transport network obstructions in the study area.

Table 1
Response times and distances under the three response conditions.

Address	Normal		Naïve Blockage Re-routing		LiDAR Assisted Blockage Re-routing	
	Time (m:ss)	Dist (mi)	Time (m:ss)	Dist (mi)	Time (m:ss)	Dist (mi)
6902 Louis XIV St.	1:21	0.8	3:42	1.9	1:34	0.8
703 Crystal St.	1:16	0.6	1:16	0.6	1:16	0.6
55 Thrasher St.	1:01	0.5	4:26	2.4	3:28	1.8
32 Heron St.	1:21	0.8	4:59	3.4	1:32	0.9
30 Tern St.	2:52	1.5	5:59	4.0	2:51	1.8
1435 Aviators St.	2:16	1.3	4:56	3.3	2:21	1.4
1755 Burbank St.	3:11	1.8	5:28	3.6	3:38	2.1
1411 Robert E Lee Blvd.	1:14	0.7	4:31	3.2	1:15	0.7
39 Lark St.	2:26	1.3	4:56	3.3	2:34	1.6
505 Mouton St.	1:29	0.8	3:47	2.0	1:42	0.9
415 Emerald St.	1:22	0.7	1:45	0.9	1:32	0.8
6015 Wickfield Dr.	3:24	1.9	7:28	4.7	3:46	2.1
99 Swan St.	1:53	0.9	6:02	4.2	2:47	1.5
1301 Jay St.	2:07	1.2	4:31	3.2	3:10	2.4
6855 Memphis St.	1:10	0.6	2:48	1.4	1:27	0.7
922 Amethyst St.	1:10	0.6	1:10	0.6	1:10	0.6
6904 General Haig St.	0:34	0.3	0:34	0.3	0:34	0.3
6419 Bertha Dr.	2:42	1.5	4:19	3.0	3:44	2.7
6900 General Diaz St.	0:54	0.5	3:11	1.6	0:58	0.5
1525 Athis St	2:56	1.6	4:37	3.1	3:15	2.3
7501 Marconi Dr.	0:56	0.5	4:08	2.2	3:22	1.8
630 Jewel St.	1:11	0.7	1:59	1.1	1:16	0.6
6532 Pratt Dr.	3:07	2.2	3:15	2.2	3:15	2.2
18 Warbler St.	1:45	0.9	3:32	1.9	2:50	1.5
1301 New York St.	1:58	1.1	3:35	2.6	3:00	2.3
6622 Spanish Fort Blvd.	1:40	0.9	1:40	0.9	1:40	0.9
1501 Killdeer St.	2:33	1.4	4:03	2.9	3:36	2.6
6220 Perlita Dr.	2:29	1.4	4:05	2.9	3:31	2.5
6000 Wildair Dr.	3:39	2.1	5:07	3.5	4:40	3.2
1701 Pressburg St.	3:10	1.8	4:17	2.9	3:47	2.6
Average	1:58	1.1	3.52	2.5	2.31	1.6

conditions where debris was present using the Naïve Blockage Re-routing; and finally under post-storm conditions using LiDAR Assisted Blockage Re-routing.

Table 1 lists the results of the routing analysis for each of the addresses. The results under normal (pre-storm) response conditions established the baseline response times and distances for

each of the random addresses. These baseline results were used to provide an initial measure of the effectiveness of incorporating the blockages detected using the LiDAR data. As shown in Table 1, the routing analysis under post-storm conditions with Naïve Blockage Re-routing resulted in an increase in average response time for the 30 routes from 1 min 58 s to 3 min 52 s. There was also an increase in average distance for the routes from 1.1 mile to 2.5 miles as compared to the baseline results. These changes amount to a 96.6% increase in average response time and a 127.3% increase in average distance for the 30 routes.

The results for the routing analysis under post-storm conditions using LiDAR Assisted Blockage Re-routing also resulted in an increase in average response time for the 30 routes from 1 min 58 s to 2 min 31 s. There was also an increase in average distance for the routes from 1.1 mile to 1.6 mile. These changes amount to a 45.5% increase in average response time and a 28.0% increase in average distance for the 30 routes. The increase in response times and distances for the LiDAR Assisted Blockage Re-routing was thus smaller than the increase for the Naïve Blockage Re-routing was used (with 1 min 21 s and 0.9 mile less). It also means that there were a 30.2% reduction in average response time and a 31.5% decrease in average distance when the LiDAR Assisted Blockage Re-routing was used when compared to using the Naïve Blockage Re-routing.

Paired *t*-tests were performed on these results to compare whether the increases in response times and distances for the 30 routes between the pre-storm response conditions and the post-storm response conditions are statistically significant. The results revealed that the post-storm response times and distances when LiDAR was not used are significantly higher than the pre-storm response times and distances (at the $p < 0.0001$ level). Further, the post-storm response times and distances when LiDAR Assisted Blockage Re-routing was used are also significantly higher than the pre-storm response times and distances (at the $p < 0.0001$ level).

Since the response times will increase if blockages are present in the street network, the difference between the normal baseline response times (or distances) and each of the two post-storm response conditions does not actually reflects the gain in using LiDAR data. In order to determine whether using LiDAR-detected blockage data is more effective than not using these detected blockages, differences in response times and distances between the two post-storm re-routing scenarios were evaluated and presented in Table 2.

As indicated in the table, the response times when LiDAR Assisted Blockage Re-routing was used were always lower than when it was not used, except in the four cases where there were no blockages present on the route between the fire station and the random location. On average the response times when LiDAR Assisted Blockage Re-routing was used were 30.2% (or 1 min 21 s) faster than when Naïve Blockage Re-routing was used (Table 2). In one case, LiDAR Assisted Blockage Re-routing reduced the response time by 72.3% (3 min 16 s). A paired *t*-test revealed a significant difference (at the $p < 0.0001$ level) in response times between the two post-storm re-routing scenarios, suggesting that response times are significantly lower when LiDAR was incorporated into the routing analysis than when LiDAR data were not used. Similar results hold for travel distances between the two post-storm response conditions. On average the travel distances when LiDAR Assisted Blockage Re-routing was used were 31.5% (0.9 mile) shorter than when Naïve Blockage Re-routing was used. In one case, LiDAR Assisted Blockage Re-routing reduced the travel distance by 78.1% (2.5 miles). Again the difference in travel distances between the two post-storm routing scenarios is statistically significant at the $p < 0.0001$ level.

Table 2
Comparison of response time increases for each post-storm routing method.

Address	Naïve Blockage Re-routing		LiDAR Assisted Blockage Re-routing		Difference	
	Time (m:ss)	Dist (mi)	Time (m:ss)	Dist (mi)	Time (m:ss)	Dist (mi)
6902 Louis XIV St.	3:42	1.9	1:34	0.8	2:08	1.1
703 Crystal St.	1:16	0.6	1:16	0.6	0:00	0.0
55 Thrasher St.	4:26	2.4	3:28	1.8	0:58	0.6
32 Heron St.	4:59	3.4	1:32	0.9	3:27	2.5
30 Tern St.	5:59	4.0	2:53	1.8	3:06	2.2
1435 Aviators St.	4:56	3.3	2:21	1.4	2:35	1.9
1755 Burbank St.	5:28	3.6	3:38	2.1	1:50	1.5
1411 Robert E Lee Blvd.	4:31	3.2	1:15	0.7	3:16	2.5
39 Lark St.	4:56	3.3	2:34	1.6	2:22	1.7
505 Mouton St.	3:47	2.0	1:42	0.9	2:05	1.1
415 Emerald St.	1:45	0.9	1:32	0.8	0:13	0.1
6015 Wickfield Dr.	7:28	4.7	3:46	2.1	3:42	2.6
99 Swan St.	6:02	4.2	2:47	1.5	3:15	2.7
1301 Jay St.	4:31	3.2	3:10	2.4	1:21	0.8
6855 Memphis St.	2:48	1.4	1:27	0.7	1:21	0.7
922 Amethyst St.	1:10	0.6	1:10	0.6	0:00	0.0
6904 General Haig St.	0:34	0.3	0:34	0.3	0:00	0.0
6419 Bertha Dr.	4:19	3.0	3:44	2.7	0:35	0.3
6900 General Diaz St.	3:11	1.6	0:58	0.5	2:13	1.1
1525 Athis St.	4:37	3.1	3:15	2.3	1:22	0.8
7501 Marconi Dr..	4:08	2.2	3:22	1.8	0:46	0.4
630 Jewel St.	1:59	1.1	1:16	0.6	0:43	0.5
6532 Pratt Dr.	3:15	2.2	3:15	2.2	0:00	0.0
18 Warbler St.	3:32	1.9	2:50	1.5	0:42	0.4
1301 New York St.	3:35	2.6	3:00	2.3	0:35	0.3
6622 Spanish Fort Blvd.	1:40	0.9	1:40	0.9	0:00	0.0
1501 Killdeer St.	4:03	2.9	3:36	2.6	0:27	0.3
6220 Perlita Dr.	4:05	2.9	3:31	2.5	0:34	0.4
6000 Wildair Dr.	5:07	3.5	4:40	3.2	0:27	0.3
1701 Pressburg St.	4:17	2.9	3:47	2.6	0:30	0.3
Average					1:21	0.9

4.3. Discussion of results

As these results indicate, using LiDAR data in post-disaster situations reduced response times and travel distances by about one-third. The best improvement can be a reduction of as much as two-thirds of the times or distances when no LiDAR data were used. This is a significant improvement from the traditional approach of simply utilizing the fastest route under normal conditions, and then deviating from that route as blockages in the roads are discovered. The results also suggest that the use of LiDAR data immediately after a storm or other disaster events has the potential to increase the number of lives saved by rescuers. LiDAR data enable rescuers to respond in a more expedient manner. In emergency situations, minutes and even seconds can make the difference between life and death for victims of a disaster. Having prior knowledge of which roads to avoid due to blockage serves to shave minutes off the time it takes for rescuers to reach victims. This study thus supports the notion that utilizing LiDAR data to supplement a GIS would be beneficial in an emergency response environment such as the situation after Hurricane Katrina.

It is important to note that because our method only identified locations with significant increase in elevation that spanned the entire street or highway, our analysis did not take into account other kinds of obstructions that could hinder travel by emergency vehicles. For instance, there may be areas that had experienced a significant decrease in elevation, and there may be other vehicles or objects that could render a road segment impassable. But they were not included as obstructions in our analysis. It is therefore likely that the number of network blockages could actually be greater than what was found using the method in this study. A more sophisticated method for determining what constitutes a blockage may have improved the results – for example, considering both significant increases and decreases in elevation, as well as taking into account volumetric change in addition to elevation change. Complementing the LiDAR data with other remotely sensed data (such as high-resolution satellite images or aerial photos) would also allow us to more accurately determine what kind of road blockages they actually were.

Further, while the results were obtained based on the assumption of free-flow traffic, it is unlikely that responders can travel at free-flow speeds right after the storm. The study has not examined how different travel speeds would affect the results. But since the spatial pattern of road blockages could be highly complex and its impact on travel speed could be rapidly changing in real-time, we have made the simplifying assumption that represents the "best scenario." If minor road blockages were widespread and there were few significant changes in the topological structure of the street network (i.e., few impassable roads), there will be a general and widespread reduction in travel speed after the storm. Lower travel speed throughout the street network would lead to longer travel times, but it would not change the shortest paths identified in the routing analysis. This situation would render the contribution of LiDAR Assisted Blockage Re-routing less important. On the other hand, if the blockages led to significant topological changes in the street network (i.e., there are many blocked roads), the time saved by LiDAR Assisted Blockage Re-routing would still be important because of its capability in identifying the shortest alternative route for reaching a given destination.

5. Conclusions

The method outlined in this article builds upon recent research on the application of LiDAR technology in disaster management (e.g., Firchau & Wiechert, 2005; Laefer & Pradhan, 2006). The results of this study show that using LiDAR data improves the speed with which emergency responders reach disaster sites. They help them to find the quickest route available instead of re-routing each time they encounter a blockage. This saves time when finding a route to a disaster site and enables responders to arrive at the scene more quickly. Shorter response times increase the likelihood that any victims of the disaster will receive aid more quickly. They also enable responders to spend less time in transit and more time assisting victims.

While this research suggests that using LiDAR data would be beneficial, there are many issues that need to be resolved if it is to be successfully implemented in real disaster situations. For instance, while the collection of LiDAR data involves using airborne equipment and takes several hours to cover a small disaster site, there are various institutional obstacles that need to be resolved beforehand if the data are to be acquired, processed, and delivered to users in a timely fashion (Bruzewicz, 2003). Companies capable of collecting and processing LiDAR data may not be willing to undertake flying missions under hazardous weather conditions, or they may be working on other contracts and cannot collect the data in a timely manner. In order to minimize the delays in data acquisition, processing, and dissemination, FEMA should work with local agencies to develop an organizational framework and procurement procedures to ensure that all necessary contracting arrangements are in place prior to the event (Bruzewicz, 2003). In addition, issues like who will capture the data, who will process them, who will analyze them, and how the data will be disseminated should be resolved beforehand (Chen et al., 2003).

Another issue is that LiDAR data need to be integrated into a comprehensive GIS database with other layers of geospatial data for them to be more useful. For instance, the analysis of transport network obstructions in this study would be more accurate if other data layers such as flood depth data or imagery of minor obstructions were used in addition to the LiDAR data. However, different pre-disaster and post-disaster data layers may use different coordinate systems, data models, and space–time resolution. They may also be collected at different times and on different dates. They may be difficult to integrate because of incompatible formats, scales, and inaccuracies (Chen et al., 2003; Cutter, 1996; Cutter, Mitchell, & Scott, 2000; Goodchild, 2003). While it is possible to convert data from one coordinate system or format to another, this is not the optimal situation for disaster response situations. For instance, because LiDAR datasets have a large number of data points, converting from one coordinate system to the other is time consuming and can take many hours. It is therefore important that pre-disaster data should be converted and integrated into a comprehensive GIS database before disaster events. The effort and time needed for data conversion and integration for post-disaster data should also be minimized.

Lastly, delivering geospatial data to emergency managers and other relevant users (e.g., Red Cross damage assessment teams) in a timely fashion also poses serious challenges. Data organization and dissemination, for instance, occurred in an ad hoc fashion in response to Katrina (Mills et al., 2008). Although there were national and state standards that specify how circumstances like this should be handled, "not all jurisdictions are equally prepared or have the capability or will to prepare according to government specifications" (Mills et al., 2008, 469). It is therefore important to establish an effective spatial data infrastructure through cooperation between governmental, academic, and commercial organizations responsible for maintaining a jurisdiction's spatial data (Tait, 2003). To ensure the needed geospatial data are well integrated and effectively disseminated, lessons can be drawn from the GIS clearinghouse model exemplified by the Louisiana State University (LSU) GIS Clearinghouse Cooperative (LGCC). The LGCC was established 5 days after Katrina wrought catastrophic destruction along the Gulf Coast through the cooperation between FEMA and Louisi-

ana State University personnel. It demonstrated how complex issues involved in data collection, analysis, organization, dissemination, and archiving may be addressed in preparation and response to a disaster (e.g., the use of Virtual Private Networks to disseminate data over the Internet securely; financial support by FEMA; and the kind of equipment and personnel needed) (Radke et al., 2000).

Acknowledgements

The authors acknowledge the Louisiana State University (LSU) GIS Clearinghouse Cooperative (http://www.katrina.lsu.edu) for making the data used in this study available. They also thank the reviewers for their helpful comments.

References

Abbas, S. H., Srivastava, R. K., Tiwari, R. P., & Bala Ramudu, P. (2009). GIS-based disaster management: A case study for Allahabad Sadar sub-district (India). *Management of Environmental Quality: An International Journal, 20*(1), 33–51.

Ahearn, S. C. (2003). Case study: GIS at the World Trade Center after September 11, 2001. In K. C. Clarke (Ed.), *Getting started with geographic information systems* (pp. 241–252). Upper Saddle River, NJ: Prentice Hall.

Aitkenhead, M. J., Lumsdon, P., & Miller, D. R. (2007). Remote sensing-based neural network mapping of tsunami damage in Aceh, Indonesia. *Disasters, 31*(3), 217–226.

Armenakis, C., & Savopol, F. (2004). *Assessment of LiDAR and digital camera data in the context of rapid change detection methodologies*. Paper presented at the XXth ISPRS Congress.

Ball, G. L., & Guertin, D. P. (1992). Improved fire growth modeling. *International Journal of Wildland Fire, 2*(2), 47–54.

Baltsavias, E. P. (1999). A comparison between photogrammetry and laser scanning. *ISPRS Journal of Photogrammetry and Remote Sensing, 54*(2–3), 83–94.

Biasion, A., Bornaz, L., & Rinaudo, F. (2005). Laser scanning applications on disaster management. In P. van Oosterom, S. Zlatanova, & E. M. Fendel (Eds.), *Geo-information for disaster management* (pp. 19–33). Berlin: Springer-Verlag.

Bruzewicz, A. J. (2003). Remote sensing imagery for emergency management. In S. L. Cutter, D. B. Richardson, & T. J. Wilbanks (Eds.), *The geographical dimensions of terrorism* (pp. 87–97). New York: Routledge.

Carrara, A., & Guzzetti, F. (Eds.). (1996). *Geographical information systems in assessing natural hazards*. Dordrecht: Kluwer.

Cahan, B., & Ball, M. (2002). GIS at ground zero: Spatial technology bolsters World Trade Center response and recovery. *GeoWorld, 15*(1), 26–29.

Center for Coastal and Watershed Studies (2007). *Hurricane Rita – Coastal change hazards: Hurricanes and extreme storms*. <http://coastal.er.usgs.gov/hurricanes/rita/> [retrieved 07.09.08].

Center for Coastal and Watershed Studies (2008a). *Hurricane Ike – Coastal change hazards: Hurricanes and extreme storms*. <http://coastal.er.usgs.gov/hurricanes/ike/> [retrieved 07.09.08].

Center for Coastal and Watershed Studies (2008b). *Hurricane Katrina – Coastal change hazards: Hurricanes and extreme storms*. <http://coastal.er.usgs.gov/hurricanes/katrina/index.html> [retrieved 07.0908].

Centre for Applied Remote Sensing Modelling and Simulation (2006). *LiDAR – Overview of technology, applications, market features and industry*. Victoria, British Columbia, Canada: University of Victoria.

Chen, K., Blong, R., & Jacobson, C. (2003). Towards an integrated approach to natural hazards risk assessment using GIS: With reference to bushfires. *Environmental Management, 31*(4), 546–560.

Chou, Y. H. (1992). Management of wildfire with a geographic information system. *International Journal of Geographical Information Systems, 6*(2), 123–140.

City of New Orleans (2008). City of New Orleans GIS Data Portal. <http://gisweb.cityofno.com/cnogis>.

Corbley, K. P. (1995). South Florida fine-tunes GIS in hurricane's aftermath. *GIS World, 8*(9), 40–43.

Cova, T. J. (1999). GIS in emergency management. In P. A. Longley, M. F. Goodchild, D. J. Maguire, & D. W. Rhind (Eds.), *Geographical information systems: Principles, techniques, applications, and management* (pp. 845–858). New York: John Wiley & Sons.

Cova, T. J., & Church, R. L. (1997). Modelling community evacuation vulnerability using GIS. *International Journal of Geographical Information Science, 11*(8), 763–784.

Curtis, A., Mills, J. W., Blackburn, J. K., & Pine, J. C. (2006). *Hurricane Katrina: GIS response for a major metropolitan area*. Boulder, CO: University of Colorado, Natural Hazards Research and Applications Information Center.

Cutter, S. L. (1996). Vulnerability to environmental hazards. *Progress in Human Geography, 20*(4), 529–539.

Cutter, S. L. (2003). GI science, disasters, and emergency management. *Transactions in GIS, 7*(4), 439–446.

Cutter, S. L., Mitchell, J. T., & Scott, M. S. (2000). Revealing the vulnerability of people and place. A case study of Georgetown County, South Carolina. *Annals of the Association of American Geographers, 90*(4), 713–734.

Dash, N. (1997). The use of geographic information system in disaster research. *International Journal of Mass Emergencies and Disasters, 15*(1), 135–146.

Dunn, C. E., & Newton, D. (1992). Optimal routes in GIS and emergency planning applications. *Area, 24*(3), 259–267.

Ertug Gunes, A., & Kovel, J. P. (2000). Using GIS in emergency management operations. *Journal of Urban Planning and Development, 126*(3), 136–149.

Firchau, S., & Wiechert, A. (2005). Accurate on-time geo-information for disaster management and disaster prevention by precise airborne LiDAR scanning. In P. van Oosterom, S. Zlatanova, & E. M. Fendel (Eds.), *Geo-information for disaster management*. Berlin: Springer-Verlag.

Goodchild, M. F. (2003). Geospatial data in emergencies. In S. L. Cutter, D. B. Richardson, & T. J. Wilbanks (Eds.), *The geographical dimensions of terrorism* (pp. 99–102). New York: Routledge.

Hoyois, P., Scheuren, J. M., Below, R., & Guha-Sapir, D. (2007). *Annual disaster statistical review: Numbers and trends 2006*. Brussels, Belgium: Catholic University of Louvain.

Huyck, C. K., & Adams, B. J. (2002). *Emergency response in the wake of the World Trade Center attack: The remote sensing perspective*. Multidisciplinary Center for Earthquake Engineering Research, University at Buffalo, State University of New York.

Kaiser, R., Spiegel, P. B., Henderson, A. K., & Gerber, M. L. (2003). The application of geographic information systems and global positioning systems in humanitarian emergencies: Lessons learned, programme implications and future research. *Disasters, 27*(2), 127–140.

Kwan, M.-P. (2003). Intelligent emergency response systems. In S. L. Cutter, D. B. Richardson, & T. J. Wilbanks (Eds.), *The geographical dimensions of terrorism* (pp. 111–116). New York: Routledge.

Kwan, M.-P., & Lee, J. (2005). Emergency response after 9/11: The potential of real-time 3D GIS for quick emergency response in micro-spatial environments. *Computers, Environment and Urban Systems, 29*(2), 93–113.

Laefer, D. F., & Pradhan, A. R. (2006). Evacuation route selection based on tree-based hazards using light detection and ranging and GIS. *Journal of Transportation Engineering, 132*(4), 312–320.

Maniruzzaman, K. M., Okabe, A., & Asami, Y. (2001). GIS for cyclone disaster management in Bangladesh. *Geographical and Environmental Modelling, 5*(2), 123–131.

Mansourian, A., Rajabifard, A., & Zoej, M. J. V. (2005). Development of a web-based GIS using SDI for disaster management. In P. van Oosterom, S. Zlatanova, & E. M. Fendel (Eds.), *Geo-information for disaster management* (pp. 599–608). Berlin: Springer-Verlag.

Mills, J. W., Curtis, A., Pine, J. C., Kennedy, B., Jones, F., Ramani, R., et al. (2008). The clearinghouse concept: A model for geospatial data centralization and dissemination in a disaster. *Disasters, 32*(3), 467–479.

Pu, S., & Zlatanova, S. (2005). Evacuation route calculation of inner buildings. In P. van Oosterom, S. Zlatanova, & E. M. Fendel (Eds.), *Geo-information for disaster management* (pp. 1143–1161). Berlin: Springer-Verlag.

Radke, J., Cova, T., Sheridan, M. F., Troy, A., Mu, L., & Johnson, R. (2000). Application challenges for geographic information science. Implications for research, education, and policy for emergency preparedness and response. *URISA Journal, 12*(2), 15–30.

Tait, M. (2003). The need for a national spatial data infrastructure. In S. L. Cutter, D. B. Richardson, & T. J. Wilbanks (Eds.), *The geographical dimensions of terrorism* (pp. 77–85). New York: Routledge.

van Oosterom, P., Zlatanova, S., & Fendel, E. M. (Eds.). (2005). *Geo-information for disaster management*. Berlin: Springer-Verlag.

United States Geological Survey (2006). Hurricane Katrina disaster response. <http://gisdata.usgs.net/hurricanes/katrina/index.php> [retrieved 12.01.08].

Walter, J. (2007). *World disasters report 2007: Focus on discrimination*. Geneva: International Federation of Red Cross and Red Crescent Societies.

Zerger, A., & Smith, D. I. (2003). Impediments to using GIS for real-time disaster decision support. *Computers, Environment and Urban Systems, 27*(2), 123–141.